Phys Chem Minerals (2002) 29: 87–97
DOI 10.1007/s002690100214

ORIGINAL PAPER

D. M. Jenkins · K. Ishida · V. Liogys · D. Ghosh

Cation distribution in amphiboles synthesized along the Ga analogue of the tremolite–aluminotschermakite join

Received: 5 March 2001 / Accepted: 31 July 2001

Abstract Amphiboles were synthesized from bulk compositions prepared along the join $Ca_{1.8}Mg_{5.2}Si_8O_{22}(OH)_2$–$Ca_{1.8}Mg_3Ga_4Si_6O_{22}(OH)_2$ hydrothermally at 750–850 °C and 1.0–1.8 GPa, and along the join $Ca_2Mg_5Si_8O_{22}F_2$–$Ca_2Mg_3Ga_4Si_6O_{22}F_2$, anhydrously at 1000 °C and 0.7 GPa to document how closely the tschermak-type substitution is obeyed in these analogues of aluminous amphiboles. Electron-microprobe analyses and Rietveld X-ray diffraction structure refinements were performed to determine cation site occupancies. The extent of Ga substitution was found to be limited in both joins, but with the fluorine series having about twice the Ga content (0.6 atoms per formula unit, apfu) of the hydroxyl-series amphiboles (0.3 apfu). The tschermak-type substitution was followed very closely in the hydroxyl series with essentially equal partitioning of Ga between tetrahedral and octahedral sites. The fluorine-series amphiboles deviated significantly from the tschermak-type substitution and, instead, appeared to follow a substitution that is close to a Ca-pargasite substitution of the type: $^{[6]}Ga^{3+} + 2^{[4]}Ga^{3+} + 1/2^{[A]}Ca^{2+} = {}^{[6]}Mg^{2+} + 2^{[4]}Si^{4+} + 1/2^{[A]}\square$. Infrared spectroscopy revealed an inverse correlation between the intensity of the OH-stretching bands and the Ga content for the hydroxyl- *and* fluorine-series amphiboles. The direct correlation between the Ga and F content and inverse relationship between the Ga and OH content may be a general phenomenon present in other minerals and suggests, for example, that high F contents in titanite are controlled by the Al content of the host rock and that there may be similar direct Al–F correlations in tschermakitic amphiboles. Evidence for the possibility that Al (Ga) might substitute onto only a subset of the tetrahedral sites in tschermakitic amphiboles was sought but not observed in this study.

Keywords Amphibole · Tschermak · Tremolite · Fluorine · Gallium

D. M. Jenkins (✉) · V. Liogys · D. Ghosh
Department of Geological Sciences and Environmental Studies,
Binghamton University,
Binghamton, New York 13902-6000, USA
Tel.: +1-607-777-2264
Fax: +1-607-777-2288
E-mail: dmjenks@binghamton.edu

K. Ishida
Kyushu University
Graduate School of Social and Cultural Studies,
4-2-1 Ropponmatsu, Chuo-ku,
Fukuoka, 810, Japan

V. Liogys
Department of Geological Sciences,
Virginia Polytechnic Institute and State University,
Blacksburg, Virginia 24061-0420, USA

Introduction

The Al–tschermak exchange, $^{[6]}Al + {}^{[4]}Al = {}^{[6]}Mg + {}^{[4]}Si$, where the superscripts indicate coordination, is widely regarded as an important exchange reaction that accounts for the incorporation of Al into many common minerals, including layered silicates (e.g., Roots 1995; Konopásek 1998) and amphiboles (e.g., Stephenson 1993; Zingg 1993). Even though this exchange reaction has been studied experimentally for various amphibole-bearing assemblages (e.g., Oba 1978; Cao et al. 1986; Jenkins 1988, 1994; Cho and Ernst 1991; Hoschek 1995; Quirion and Jenkins 1998), there are few studies that have included information on the distribution of Al between the octahedral and tetrahedral sites. That is to say, there are relatively few studies that have actually verified how closely the tschermak substitution is obeyed. This stems largely from the inability to easily distinguish the locations of Al, Si, and Mg in the crystal structure because of their very similar X-ray scattering powers. Recent single-crystal X-ray refinements have made important advances in deducing the distribution of Al in octahedral and tetrahedral sites of natural (chemically more complex) amphiboles using bond-distance and ionic-radii correlations (Oberti et al. 1995a, b), especially when used in conjunction with bond-valence

theory (Hawthorne 1997). Single-crystal studies of synthetic (chemically simpler) amphiboles are usually not feasible because of their extremely fine grain sizes. Infrared and MAS–NMR analyses (Jenkins et al. 1997; Hawthorne et al. 2000) have also contributed to our understanding of the distribution of cations in aluminous amphiboles, but these spectroscopic techniques are more effective at offering support for proposed models rather than providing definitive results.

An alternative approach to deducing the distribution of aluminum in amphiboles is to study gallium analogues, whereby the enhanced scattering power of gallium compared to that of magnesium and silicon facilitates determination of its occupancy at a given site. This approach was used by Jenkins and Hawthorne (1995) in the study of Ga-bearing amphiboles which had been synthesized from bulk compositions incorporating the pargasite exchange (= Al-tschermak + edenite exchange). In the study by Jenkins and Hawthorne (1995), the cation distribution of synthetic amphiboles was deduced using the Rietveld technique applied to X-ray diffraction powder patterns. In the present study, we attempt to discern the distribution of Ga in amphiboles synthesized from bulk compositions incorporating the Al-tschermak substitution alone.

Experimental and analytical techniques

Apparatus

In accord with previous studies of aluminotschermakite synthesis (e.g., Jenkins 1988; Cho and Ernst 1991), syntheses of hydroxyl-bearing amphiboles were performed in the pressure range of 1.0–1.7 GPa using a 1/2-inch diameter piston-cylinder press. The piston-cylinder press employed an NaCl pressure-medium assemblage. A detailed discussion of the calibration of pressures at the sample position inside the pressure medium is given in Quirion and Jenkins (1998). The precision of pressure measurement is estimated at ±0.03 GPa. Temperatures were measured with chromel-alumel thermocouples with an approximate uncertainty of ±5 °C.

Fluorine-bearing amphiboles were synthesized at about 0.7 GPa inside internally heated gas vessels using Ar gas as the pressure medium. Temperatures were recorded with dual Inconel-sheathed chromel-alumel thermocouples positioned near each end of the sample. Temperature uncertainty in these runs included thermocouple accuracy (±2 °C), controller variation (±1 °C), and any thermal gradient across the sample. Pressures were monitored with a Bourdon-tube gauge and Harwood manganin cell and were considered accurate to ±0.005 GPa.

Phase synthesis

All syntheses were made from stoichiometric proportions of the following oxides and carbonates: MgO, Ga_2O_3, SiO_2 (derived from silicic acid), $CaCO_3$, and CaF_2. Mixtures containing carbonate were roasted briefly (~30 s) at ~900 °C to drive off CO_2. For hydroxyl-bearing amphiboles, about 200 mg of the starting mixture was loaded into a Pt capsule that was annealed at 1550 °C (necessary to prevent capsule rupture), roasted briefly at ~900 °C to drive off CO_2, and sealed with 20 wt% water. For fluorine-bearing amphiboles, about 200 mg of starting mixture was loaded into $Ag_{50}Pd_{50}$ capsules and roasted briefly to ~600 °C just prior to sealing to ensure that all moisture was driven off. These mixtures were treated under the *P–T* conditions listed in Table 1.

X-ray diffraction

Powder X-ray diffraction step scans were performed on a Philips PW3040-MPD automated diffractometer operated at 40 kV and 40 mA and in the theta-theta configuration. Structure refinements of the powder patterns were performed using the Rietveld full-pattern refinement method using the DBWS-9411 software (Young et al. 1994). The diffractometer was calibrated against silicon (a_o = 5.4308 Å). Intensities were collected from 8–100° 2Θ at 0.05° steps for counting times of 5 s to give about 1000 counts on the strongest peaks. Fixed divergence and receiving slits of 1/2° were used. The powdered sample was mounted in a 8 × 20 × 1-mm rectangular Plexiglas holder backed by a glass plate. The surface of the sample was roughed up slightly with beam-parallel striations using a razor blade, as discussed in Raudsepp et al. (1990), in order to minimize grain-preferred orientation effects at the surface. Refinements were performed using the same sequence of steps as that used in Jenkins and Hawthorne (1995).

Table 1 Nominal composition, synthesis conditions, and synthesis products, arranged by increasing Ga content

Sample	Nominal composition	*T* (°C)	*P* (GPa)	*t* (h)	Products (wt%)[a]					
					Amph	Qtz	Cpx	Sapph	Opx	Fluorite
OH series										
AM1L2	$Ca_{1.8}Mg_{5.2}Si_8O_{22}(OH)_2$	850 (10)[b]	1.50 (3)	168	99 (2)	0.7 (1)	–	–	–	–
AM5B-1	$Ca_{1.8}Mg_{5.1}Ga_{0.2}Si_{7.9}O_{22}(OH)_2$	800 (10)	1.00 (3)	144	100	–	–	–	–	–
AM10B-1	$Ca_{1.8}Mg_{5.0}Ga_{0.4}Si_{7.8}O_{22}(OH)_2$	800 (10)	1.20 (3)	164	89 (2)	–	6.4 (2)	–	4.4 (2)	–
AM15B-1	$Ca_{1.8}Mg_{4.9}Ga_{0.6}Si_{7.7}O_{22}(OH)_2$	800 (10)	1.40 (3)	118	95 (2)	–	1.0 (2)	3.9 (2)	–	–
AM2Va	$Ca_{1.8}Mg_{4.8}Ga_{0.8}Si_{7.6}O_{22}(OH)_2$	800 (10)	1.66 (3)	167	92 (2)	–	3.2 (2)	4.9 (2)	–	–
AM3f	$Ca_{1.8}Mg_{4.6}Ga_{1.2}Si_{7.4}O_{22}(OH)_2$	800 (10)	1.63 (3)	192	83 (2)	3.1 (2)	5.9 (2)	7.8 (2)	–	–
AM4d	$Ca_{1.8}Mg_{4.4}Ga_{1.6}Si_{7.2}O_{22}(OH)_2$	750 (10)	1.75 (5)	185	68 (2)	–	15.4 (3)	16.2 (2)	–	–
F series										
TREM 19-4	$Ca_2Mg_5Si_8O_{22}F_2$	998 (4)	0.712 (5)	191	96 (1)	2.1 (4)	1.2 (2)	–	–	0.6 (1)
AMPH 33-1	$Ca_2Mg_{4.8}Ga_{0.4}Si_{7.8}O_{22}F_2$	998 (4)	0.720 (5)	96	95 (2)	5.1 (4)	–	–	–	–
AMPH 30-3	$Ca_2Mg_{4.6}Ga_{0.8}Si_{7.6}O_{22}F_2$	1001 (3)	0.720 (5)	138	83 (2)	10.5 (5)	1.5 (2)	3.9 (2)	–	1.0 (1)
AMPH 34-1	$Ca_2Mg_{4.4}Ga_{1.2}Si_{7.4}O_{22}F_2$	986 (15)	0.711 (5)	191	71 (2)	14.9 (4)	3.7 (2)	9.0 (2)	–	1.1 (1)
AMPH 32-1	$Ca_2Mg_{4.2}Ga_{1.6}Si_{7.2}O_{22}F_2$	1000 (5)	0.693 (6)	73	61 (1)	18.5 (7)	5.5 (3)	12.8 (2)	–	1.7 (1)

[a] wt% via Rietveld analysis. Abbreviations: *Amph* amphibole; *Cpx* clinopyroxene; *Opx* orthopyroxene; *Qtz* quartz; *Sapph* Ga-sapphirine
[b] Note: uncertainties in the last decimal place given in parentheses

Electron-microprobe analysis

Electron-microprobe analyses were obtained on a JEOL 8900 Superprobe operated at 15 kV and 10 nA using both energy-dispersive (EDS) and wavelength-dispersive (WDS) spectrometries. Fluorine was analyzed by WDS using a 10-s counting time, to minimize F migration under the electron beam (e.g., Stormer et al. 1993), and using Wilberforce apatite (3.70 wt% F) for a standard. All other elements were analyzed by EDS using diopside as the standard for Ca, Mg, and Si, and synthetic GaP as the standard for Ga. Owing to the small sizes (1–2 μm diameter) the grains were dispersed on polished graphite stubs to ensure that free-standing grains could be identified for analysis. Analytical totals were generally less than 100 wt% because the excitation volume of the beam often exceeded the volume of the grain. We accepted amphibole compositions if they yielded analytical totals of 70 wt% or higher and cation totals of 15.0 ± 0.1 apfu on the basis of 23 oxygens for OH-bearing amphiboles. For F-bearing amphiboles, these criteria had to be altered slightly to analytical totals of 70 wt% and cation totals greater than 14.9 apfu, as discussed below.

IR spectroscopy

Infrared spectra were recorded (at Kyushu University) in the range of 3800–3000 cm^{-1} with a JASCO FTIR-620 spectrometer equipped with a DLATGS detector and a KBr beam splitter. A total of 128 scans per sample were performed in an evacuated sample chamber at a nominal resolution of 1 cm^{-1}. Samples were prepared for infrared spectroscopy by combining about 200 mg of KBr with 1.5–3.0 mg of fine-grained amphibole and pressing the mixture into 10-mm diameter disks.

Results

Sample description

Bulk compositions were prepared along the joins $Ca_{1.8}Mg_{5.2}Si_8O_{22}(OH)_2$–$Ca_{1.8}Mg_3Ga_4Si_6O_{22}(OH)_2$ and $Ca_2Mg_5Si_8O_{22}F_2$–$Ca_2Mg_3Ga_4Si_6O_{22}F_2$. The former join was purposely prepared with 1.8 Ca rather than the ideal 2.0 Ca in an attempt to optimize the amphibole yield, as suggested by the work of Jenkins (1987). The more recent study of Gottschalk et al. (1999) indicates that the optimal Ca content would be closer to 1.9 Ca [i.e., 95 mol% $Mg_7Si_8O_{22}(OH)_2$ content]. Although this level of Ca in tremolitic amphiboles formed hydrothermally in the range of 800–850 °C and 0.5–1.3 GPa has not been observed by the first author (e.g., Table 2), the exact concentration of Ca in the M4 site is considered of minor importance to this study. Here, we are examining the gallium-tschermak substitution which involves cation exchanges on the octahedral and tetrahedral sites and not on the eight-coordinated M4 site.

Reconnaissance experiments quickly showed that the full Ga analogues of aluminotschermakite (Ga-bearing end members of the above series) could not be made. The bulk compositions shown in Table 1 are grouped towards the Ga-poor ends of either join, with the maximum nominal Ga content investigated here corresponding to 1.6 apfu. The conditions at which these mixtures were treated are listed in Table 1, with the OH series on the top half and the F series on the bottom half of the table. Also listed in Table 1 are the products of synthesis listed by weight % as determined by Rietveld refinement. One can see by inspection of Table 1 that the mixtures with little or no Ga produce essentially pure amphibole yields. At Ga contents of about 0.6–0.8 apfu, the Ga analogue of sapphirine appears, which essentially marks the saturation of amphibole in Ga. Both the OH and the F series showed marked drops in the amphibole yields for Ga contents above about 0.8 Ga apfu.

For the purposes of the Rietveld refinements, the clinopyroxene was assumed to be pure diopside and the orthopyroxene to be pure enstatite. The structural data for diopside and enstatite were taken from Levien and Prewitt (1981) and Sasaki et al. (1982), respectively. All amphiboles were refined in space group $C2/m$, though one refinement was attempted in $P2/a$ (see *Discussion* below). As with the study of Jenkins and Hawthorne (1995), the dominant gallium-rich phase encountered in this study is a triclinic ($P1$), gallium analogue of sapphirine. This phase can experience a wide range of solid solution, as reported previously by Smart and Glasser (1978) for sapphirines formed in the system MgO–Ga_2O_3–SiO_2 and by Barbier (1998) for those formed in the system MgO–Ga_2O_3–GeO_2. The approach taken in this study was to model the structure of this complex phase by X-ray diffraction methods sufficient to account for its presence in the powder diffraction pattern. To this end, the structure adopted here was that of the triclinic sapphirine reported by Barbier (1998), while the Ga/Si ratios in the T1–T6 sites, the Mg/Ga ratios in the M1–M3 and M7–M9 sites, and the Mg/Ca ratios in the M4–M6 sites were refined using the most sapphirine-rich sample encountered in this study (AM4d, Table 1). The resulting composition of the sapphirine is $(Ca_{1.2}Mg_{2.0}Ga_{0.8})(Mg_{0.2}Ga_{3.8})(Ga_{4.6}Si_{1.4})O_{20}$ and the cell dimensions, using the axis orientation of Barbier (1998), are approximately $a = 8.788$, $b = 9.746$, $c = 10.223$ Å, $\alpha = 63.85°$, $\beta = 84.68°$, and $\gamma = 65.38°$. The cell dimensions of the sapphirine were refined in each synthesis mixture to provide some accommodation for minor compositional changes in the sapphirine from one mixture to the next.

Electron-microprobe analyses of amphibole

Electron-microprobe analyses of amphiboles formed in the hydroxyl-series syntheses are listed in Table 2. Figure 1 illustrates the electron-microprobe analysis (EMPA, squares) results for the observed Ga content (apfu) in amphibole as a function of the nominal Ga content of the starting mixture. It is evident in Fig. 1 that the amphiboles quickly become saturated in Ga at about 0.3 apfu, even though the nominal Ga content of the amphibole starting mixtures shown in this figure goes up to 0.6 apfu. Saturation in Ga corresponds closely with the appearance of sapphirine in the synthesis products (AM15B-1, Table 1). The partitioning of Ga between tetrahedral and octahedral sites, as deduced from the microprobe analyses, is shown in Fig. 2 (EMPA,

Table 2 Electron microprobe analyses (wt%) of the amphiboles in lowest Ga-contented mixtures of the hydroxyl-bearing series

Sample	AM1L2	AM5B-1	AM10B-1	AM15B-1
No. of analyses	8	9	13	14
SiO_2	51 (8)	50 (7)	55 (3)	55 (5)
Ga_2O_3	0.2 (2)	2.5 (8)	3.1 (12)	3.4 (6)
MgO	23 (4)	22 (4)	24 (2)	24 (3)
CaO	11 (1)	10.4 (9)	12 (1)	11.4 (7)
Sum	85 (12)	84 (13)	94 (6)	93 (9)
Cations[a]				
Si	7.96 (5)	7.88 (11)	7.86 (7)	7.84 (7)
Ga-T	0.02 (2)	0.12 (10)	0.14 (7)	0.16 (7)
Ga-C	0.0	0.13 (6)	0.14 (8)	0.15 (7)
Ga total	0.02 (2)	0.25 (6)	0.28 (10)	0.31 (4)
Mg-C	4.99 (1)	4.83 (12)	4.84 (9)	4.85 (7)
Mg-total	5.28 (11)	5.07 (26)	5.09 (22)	5.09 (12)
Mg-B	0.28 (12)	0.24 (15)	0.25 (17)	0.24 (10)
Ca-B	1.72 (12)	1.73 (17)	1.73 (17)	1.73 (10)
Ca total	1.78 (12)	1.78 (19)	1.77 (21)	1.76 (10)
Ca-A	0.06 (7)	0.05 (5)	0.05 (5)	0.03 (4)
Total cations	15.03 (4)	14.99 (9)	15.00 (6)	15.00 (7)

[a] Cations calculated on the basis of 23 oxygens

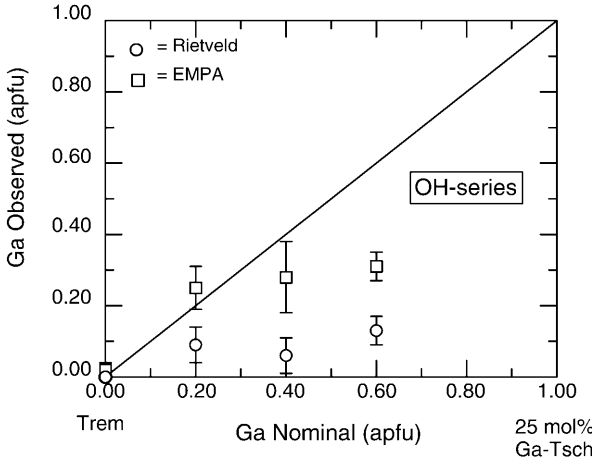

Fig. 1 Observed Ga content (atoms per formula unit = apfu) of the amphiboles formed in the OH-series syntheses vs. the nominal Ga content of the bulk starting-mixture composition. Site occupancies come from Rietveld refinements (*circles*) and from electron microprobe analyses (*squares*, EMPA). *Diagonal line* represents the 1:1 correspondence. *Error bars* in this and subsequent figures represent 1σ uncertainty

squares). Based on the microprobe results, the partitioning of Ga between octahedral and tetrahedral sites adheres closely to the expected 1:1 tschermak exchange.

Electron-microprobe analyses of amphibole grains formed in the fluorine-series syntheses are listed in Table 3. Since variable amounts of fluorine were detected by the microprobe and corresponding variations in the intensities of the infrared OH-stretching bands (see below), one cannot simply calculate the number of cations on an assumed number of oxygens. In the absence of reliable analyses of the water content of the amphibole grains, two approaches towards calculating the cations

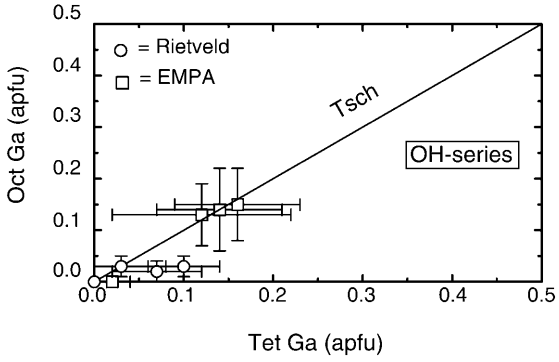

Fig. 2 Octahedral and tetrahedral Ga contents for the OH-series syntheses. *Diagonal line* represents the equipartitioning of octahedral and tetrahedral Ga expected for the tschermak (*Tsch*) substitution

were tried in this study. Calculations were first made by adjusting the total number of oxygen and fluorine anions [$\sum$(O + F)] until the sum of all cations was 15.00. It was found that the $\sum$(O + F) had to be *reduced* with increasing Ga content to maintain a constant 15.00 cations, implying increasing water content with increasing Ga content, which is contrary to what is observed (see below). An alternative approach was then taken whereby a value for the $\sum$(O + F) was found by iteration which produced a constant value for the directly measured F content. This required only two iterations at most because the number of F anions is not strongly dependent on the initial estimate of the $\sum$(O + F). The resultant values of $\sum$(O + F) shown in Table 3 increase with increasing Ga content, i.e., decreasing water content, as required by the IR spectra. A result of this calculation procedure is that there can actually be more that 15.0 cations, with some Ca appearing on the A site. Although Ca is not customarily assigned to the A site, its presence on the A site is supported here by the Rietveld refinements (discussed below) and was documented earlier by Oberti et al. (1997) in their study of synthetic fluor-pargasite.

Figure 3 illustrates the electron-microprobe analysis (EMPA, squares) results for the fluorine-series amphiboles as a function of the nominal Ga content of the starting mixture. Again the F-bearing amphiboles quickly become saturated in Ga; however, the F-bearing amphiboles become saturated at about 0.6–0.7 Ga apfu, or about twice the level of the hydroxyl series. As with the OH series, saturation in Ga corresponds closely with the appearance of sapphirine in the synthesis products (AMPH 30-3, Table 1). The partitioning of Ga between tetrahedral and octahedral sites, as deduced from the microprobe analyses, is shown in Fig. 4 (EMPA, squares). There is a distinct enrichment of tetrahedral over octahedral Ga, with all of the Ga-bearing amphiboles lying well below the solid line corresponding to the 1:1 partitioning anticipated for the tschermak substitution. Instead, the partitioning is much closer to the dashed line corresponding to the 1:2 partitioning expected for a pargasite-type substitution.

Table 3 Electron microprobe analyses (wt%) of synthetic amphiboles in the fluorine-bearing series

Sample	TREM 19-4	AMPH 33-1	AMPH 30-3	AMPH 34-1	AMPH 32-1
No. of analyses	8	11	12	11	7
SiO_2	56 (3)[b]	53 (3)	50 (5)	53 (2)	52 (4)
Ga_2O_3	0.1 (2)	3.7 (8)	6 (2)	6 (2)	8 (2)
MgO	24 (2)	23 (2)	23 (2)	24 (2)	24 (3)
CaO	12.7 (4)	12.7 (10)	12.2 (6)	12.8 (9)	12.9 (6)
F	2.4 (5)	2.7 (9)	2.7 (9)	3.4 (10)	3.2 (8)
Sum O = F	94 (5)	93 (6)	91 (7)	98 (5)	98 (9)
Cations[a]					
Si	7.99 (6)	7.76 (12)	7.58 (23)	7.56 (14)	7.41 (19)
Ga-T	0.00 (1)	0.23 (10)	0.41 (23)	0.42 (13)	0.58 (19)
Ga-C	0.01 (1)	0.12 (11)	0.16 (13)	0.15 (11)	0.15 (9)
Ga total	0.01 (1)	0.35 (7)	0.57 (23)	0.56 (18)	0.73 (19)
Mg-C	4.97 (7)	4.83 (13)	4.84 (14)	4.85 (16)	4.82 (13)
Mg total	5.06 (11)	4.99 (20)	4.98 (17)	5.14 (11)	5.08 (27)
Mg-B	0.09 (9)	0.15 (11)	0.14 (13)	0.29 (17)	0.26 (16)
Ca-B	1.87 (8)	1.84 (11)	1.86 (12)	1.71 (17)	1.73 (16)
Ca total	1.94 (11)	2.00 (13)	1.99 (10)	1.93 (7)	1.99 (15)
Ca-A	0.06 (8)	0.16 (10)	0.14 (14)	0.22 (14)	0.26 (7)
F	1.07 (18)	1.24 (37)	1.31 (7)	1.52 (42)	1.46 (27)
$\sum$(O + F)	23.54	23.66	23.65	23.82	23.74
Total cations	15.00 (7)	15.10 (13)	15.13 (15)	15.21 (16)	15.22 (12)

[a] Cations calculated on the basis of $\sum$(O + F), given in the next to the last row of the table. See text for full discussion

[b] Note: uncertainties in the last decimal place given in parentheses

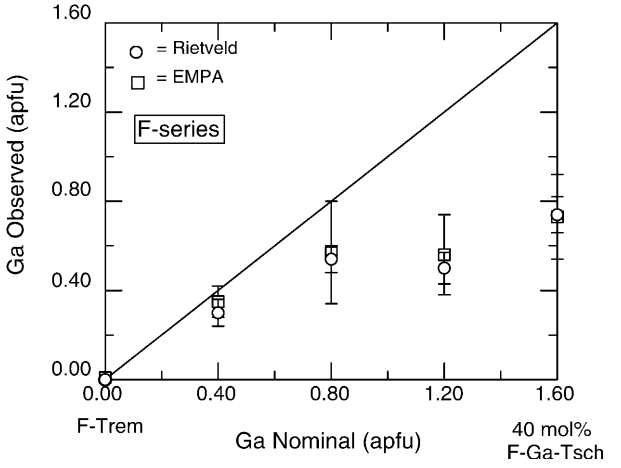

Fig. 3 Observed Ga content of the amphiboles formed in the F-series syntheses vs. the nominal Ga content of the bulk starting-mixture composition. *Diagonal line* represents the line of 1:1 correspondence

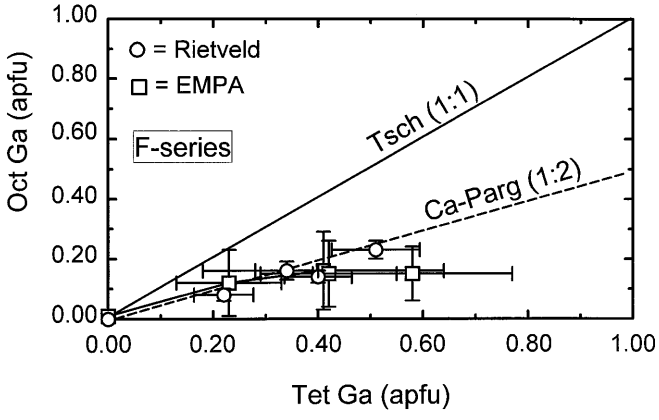

Fig. 4 Octahedral and tetrahedral Ga contents for the F-series syntheses. *Solid diagonal line* represents the equipartitioning of octahedral and tetrahedral Ga expected for the tschermak substitution [*Tsch (1:1)*], whereas the *dashed diagonal line* represents the 1:2 partitioning expected for the Ca-pargasite substitution [*Ca-Parg (1:2)*], as discussed in the text

Rietveld structure refinements of amphiboles

X-ray diffraction Rietveld structural refinements were performed for all of the mixtures investigated in this study. Agreement indices are reported in Table 4. Cation site occupancies are reported in Table 5 only for those hydroxyl- and fluorine-bearing amphiboles for which microprobe analyses have been determined. Direct refinement of the cation site occupancies was possible because of the strong X-ray scattering contrast between Ga, Mg, and Si. Refinements were performed initially allowing the Ga occupancy at both the T1 and T2 tetrahedral sites to refine as well as on all of the M1, M2, and M3 octahedral sites. In all cases Ga refined to essentially zero occupancy at the M3 and M1 sites and displayed only minor occupancies at the T2 sites.

There is excellent agreement between the Rietveld and microprobe analyses for the total observed Ga (sum of octahedral and tetrahedral Ga) for the F series, as shown in Fig. 3 (circles). It is important to stress that these two analytical techniques, Rietveld structure refinement and electron microprobe analysis, are completely independent of each other. That is to say, the total Ga content of the amphibole obtained in the Rietveld refinement was *not* restricted to match that of the microprobe analyses. The agreement between the Rietveld and microprobe results for the OH-series

Table 4 Rietveld structure refinement agreement indices. Abbreviations as in Table 1

Sample	Whole pattern indices					Individual phase indices (R_B[f])					
	R_p[a]	R_{wp}[b]	R_{exp}[c]	S[d]	D[e]	Amph	Qtz	Cpx	Sapph	Opx	Fluorite
OH series											
AM1L2	13.1	17.4	11.2	1.53	1.20	6.54	16.3	–	–	–	–
AM5B-1	12.6	16.8	12.7	1.30	1.27	5.69	–	–	–	–	–
AM10B-1	12.8	17.0	12.6	1.32	1.74	5.40	–	9.2	–	12.4	–
AM15B-1	13.1	16.9	12.3	1.36	1.55	6.60	–	11.5	14.4	–	–
AM2Va	13.2	17.2	11.5	1.47	1.28	7.45	–	10.4	13.6	–	–
AM3f	13.3	17.5	11.7	1.47	1.50	7.33	10.4	10.0	12.7	–	–
AM4d	12.3	16.6	11.7	1.40	1.27	5.70	–	7.7	10.0	–	
F series											
TREM 19-4	12.9	18.2	13.2	1.36	1.39	6.88	14.3	17.3	–	–	13.0
AMPH 33-1	12.0	16.7	13.1	1.26	1.32	5.53	20.3	–	–	–	–
AMPH 30-3	12.0	16.2	12.4	1.28	1.64	5.07	15.7	11.1	15.5	–	10.2
AMPH 34-1	12.6	17.0	12.2	1.36	1.42	4.77	16.9	10.0	12.5	–	6.9
AMPH 32-1	12.3	16.3	12.2	1.32	1.31	4.86	13.2	9.0	10.1	–	10.0

[a] R_p whole-pattern agreement index
[b] R_{wp} whole-pattern agreement index weighted by the value of counts^{-1}
[c] R_{exp} expected whole-pattern agreement index
[d] S Goodness of fit ($= R_{wp}/R_{exp}$)
[e] D Durbin-Watson D statistic
[f] R_B agreement index for Bragg reflections (includes background counts)

Table 5 Amphibole cation site occupancies (apfu) determined from Rietveld analysis. Note: In all cases the M3 site is fully occupied by Mg

Sample	T1		T2		M1		M2		M4		A
	Ga	Si	Ga	Si	Ga	Mg	Ga	Mg	Ca	Mg	Ca
OH series											
AM1L2	0	4	0	4	0	2	0	2	1.77 (6)	0.23 (6)	–
AM5B-1	0.07 (5)	3.93 (5)	0	4	0.02 (2)	1.98 (2)	0	2	1.78 (6)	0.22 (6)	–
AM10B-1	0.03 (5)	3.97 (5)	0	4	0	2	0.03 (2)	1.97 (2)	1.65 (6)	0.35 (6)	–
AM15B-1	0.10 (4)	3.90 (4)	0	4	0	2	0.03 (2)	0.97 (2)	1.73 (6)	0.27 (6)	–
F series											
TREM 19-4	0	4	0	4	0	2	0	2	1.89 (5)	0.11 (5)	0.07 (1)
AMPH 33-1	0.22 (4)	3.78 (4)	0.00 (4)	4.00 (4)	0	2	0.08 (2)	1.92 (2)	1.88 (6)	0.12 (6)	0.15 (2)
AMPH 30-3	0.26 (5)	3.74 (5)	0.14 (4)	3.86 (4)	0	2	0.14 (2)	1.86 (2)	1.93 (7)	0.07 (7)	0.10 (1)
AMPH 34-1	0.34 (6)	3.66 (6)	−0.02 (5)	4.02 (4)	0	2	0.16 (3)	1.84 (3)	1.84 (8)	0.16 (8)	0.08 (2)
AMPH 32-1	0.41 (6)	3.59 (6)	0.10 (6)	3.90 (6)	0	2	0.24 (3)	1.76 (3)	1.84 (9)	0.16 (9)	0.20 (2)

amphiboles is much worse (Fig. 1), with the Rietveld analyses yielding a Ga content of about 0.2 apfu less than that indicated by the microprobe analyses. The cause of this discrepancy is unclear but is probably related to the much lower Ga content of the OH-series amphiboles.

The Ga contents in octahedral and tetrahedral sites are indicated in Fig. 2 for the OH series and in Fig. 4 for the F series. Again, the agreement between the Rietveld and microprobe analyses is much better for the F series compared to the OH series. What is most striking is that both the microprobe analyses and Rietveld refinements support the large amount of tetrahedral vs. octahedral Ga in the F series, with close adherence to the 1:2 partitioning expected for a pargasite-type substitution. The site occupancies of the OH-series amphiboles deduced from Rietveld refinements are ambiguous because of their very low levels and relatively large uncertainties, as shown in Fig. 2. This indicates a practical lower limit of 0.15 Ga apfu for reliable detection by the Rietveld method used in this study.

Additional support for the limited substitution of Ga into either the fluorine- or hydroxyl-bearing amphiboles can be seen in the unit-cell dimension data. Table 6 lists the unit-cell dimensions for the same hydroxyl- and fluorine-series amphiboles as reported in Table 5. Figure 5 shows the cell dimensions of the hydroxyl-bearing series of amphiboles plotted against the nominal Ga contents of the mixtures. The vertical dashed line on Fig. 5 indicates where gallium sapphirine begins to appear in the synthesis products. The solid lines in Fig. 5 are drawn to suggest possible straight-line fits to the regions of the graph where amphiboles are either under- or oversaturated in gallium, as indicated by the absence

Table 6 Unit-cell dimensions of amphiboles

Sample	a (Å)	b (Å)	c (Å)	β (°)	V (Å^3)
OH series					
AM1L2	9.8080 (5)	18.051 (1)	5.2770 (3)	104.563 (4)	904.3 (1)
AM5B-1	9.8123 (6)	18.051 (1)	5.2794 (3)	104.628 (4)	904.8 (1)
AM10B-1	9.8100 (5)	18.052 (1)	5.2816 (3)	104.619 (4)	905.0 (1)
AM15B-1	9.8146 (4)	18.052 (1)	5.2807 (3)	104.653 (3)	905.2 (1)
F series					
TREM 19-4	9.8043 (3)	18.021 (1)	5.2657 (2)	104.649 (3)	900.1 (1)
AMPH 33-1	9.8121 (5)	18.025 (1)	5.2759 (3)	104.696 (4)	902.6 (1)
AMPH 30-3	9.8160 (5)	18.021 (1)	5.2794 (3)	104.736 (4)	903.2 (1)
AMPH 34-1	9.8140 (6)	18.018 (1)	5.2780 (3)	104.735 (5)	902.6 (1)
AMPH 32-1	9.8168 (6)	18.020 (1)	5.2820 (4)	104.737 (5)	903.7 (1)

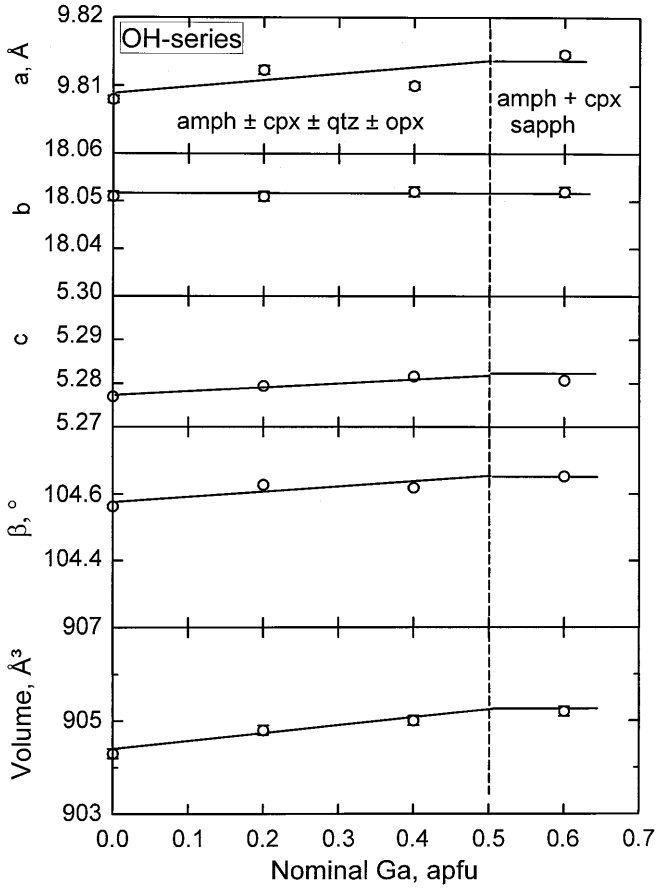

Fig. 5 Unit-cell dimensions and volumes of the amphiboles formed in the OH series. *Solid lines* are linear fits to the data while the *vertical dashed line* shows the bulk composition where sapphirine (Ga saturation) first appears

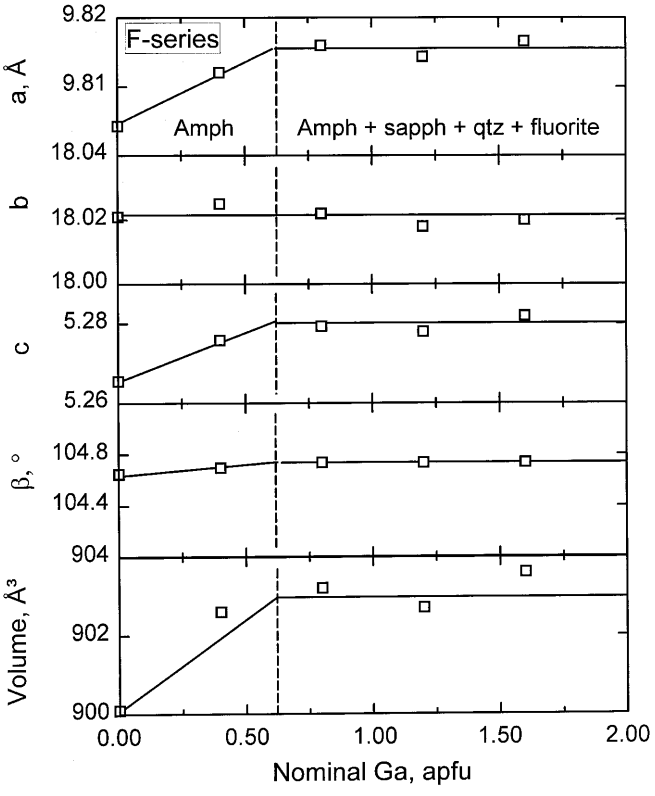

Fig. 6 Unit-cell dimensions and volumes of the amphiboles formed in the F series. *Solid lines* are linear fits to the data while the *vertical dashed line* shows the bulk composition where sapphirine (Ga saturation) first appears

or presence, respectively, of gallium sapphirine. There are slight increases in the a and c parameters and volume, which may be caused by the substitution of the larger Ga^{3+} ion for Si^{4+} into the tetrahedral chain. There is very little change in either the b or β parameters, suggesting that these parameters are insensitive to the substitution of Ga into the structure. The cell dimensions of the fluorine-bearing series are shown in Fig. 6. This figure is plotted in the same fashion as Fig. 5, where the vertical dashed line indicates the onset of sapphirine (saturation in Ga), which, incidentally, occurs at about the same Ga content as for the hydroxyl series, and the solid lines are straight-line segments to the Ga-poor and Ga-rich portions of the diagram. One can see from Fig. 6 that the effect of Ga substitution in the fluorine series produces essentially the same results (increase in a, c, and volume; little change in b and β) as in the hydroxyl series; however, the magnitude of change in the fluorine-bearing series is larger owing to the greater extent of Ga substitution.

Atomic coordinates were also refined during the Rietveld structure refinements. The calculated bond distances are in general agreement with those given in previously reported crystal refinements; unfortunately,

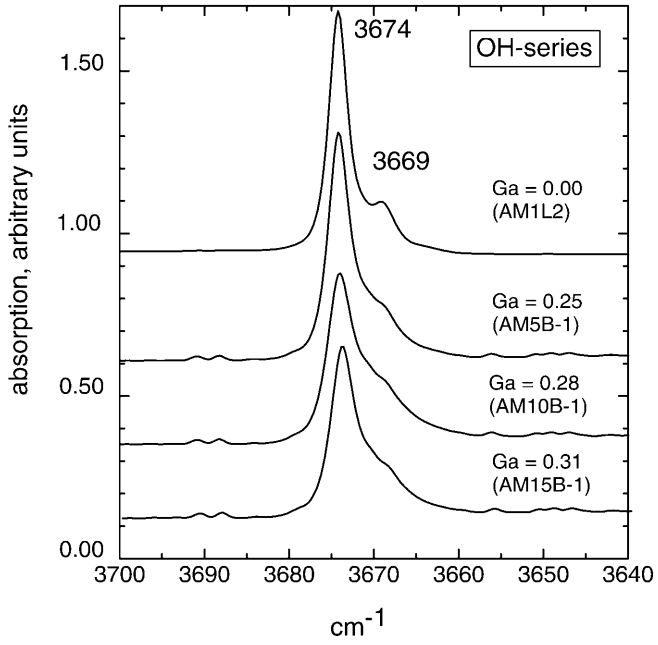

Fig. 7 Infrared spectra in the region of the OH-stretching wavenumber for amphiboles formed in the OH series. The observed Ga contents (apfu) are listed along with the sample codes. The wavenumbers of the two readily resolved bands in the tremolitic amphibole (AM1L2) are shown in the *top spectrum*. All spectra are plotted at the same scale but offset for clarity. Notice the reduction in intensity and broadening of the bands with increasing Ga content

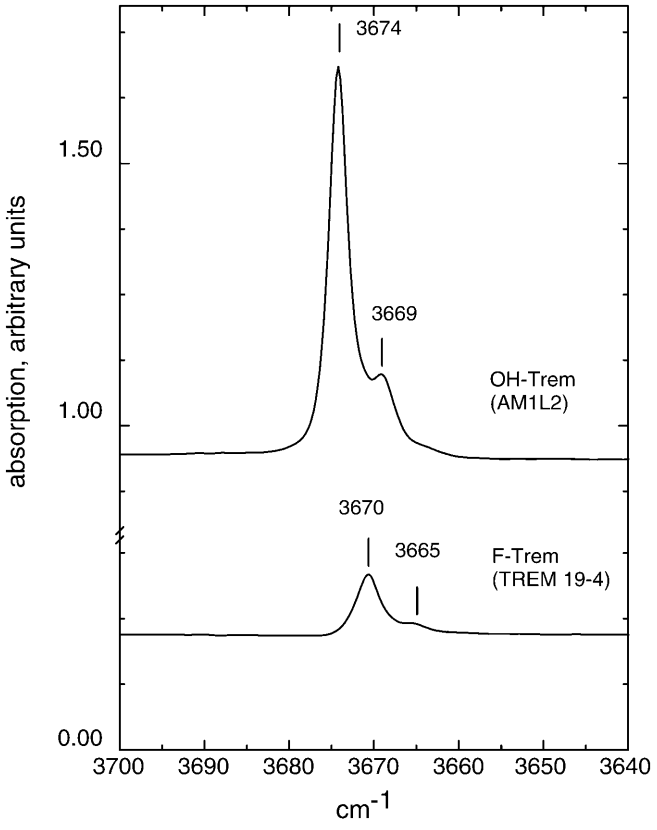

Fig. 8 Infrared spectra in the region of the OH-stretching wavenumber for Ga-free amphiboles in the OH-series (*top*) and F-series (*bottom*) syntheses. Both spectra are plotted at the same scale but offset for clarity. Note the pronounced reduction in intensity and shift to lower wavenumbers for the two readily discernible bands going from the OH- to the F-tremolite

the level of precision in the bond distances from Rietveld refinements is about an order of magnitude worse than what one obtains from single-crystal refinements (e.g., Raudsepp et al. 1990; Jenkins et al. 1997). This fact coupled with the small level of Ga substitution into either amphibole series, makes correlations between bond distances (or angles) with composition of limited significance.

Infrared spectroscopy

Since infrared spectroscopy is sensitive to the degree of short-range order about the OH anion at the O3 site, a careful inspection of these spectra may reveal additional information about the cation distributions in the amphiboles synthesized in this study. Infrared spectra were collected for both the hydroxyl- *and* fluorine-bearing series in the region of the OH-stretching vibration and are shown in Figs. 7–9.

Hydroxyl-series syntheses

The spectra of the OH-bearing amphiboles analyzed by the microprobe (Table 3) are shown in Fig. 7. Notice that each of the spectra in this figure and in Figs. 8 and 9 are plotted at the same relative scale but have been offset for clarity. The top spectrum in Fig. 7 is for AM1L2, essentially OH-tremolite, and has a sharp and intense band centered at 3674 cm^{-1} and a small but distinct shoulder band at 3669 cm^{-1}. The 3674 cm^{-1} band has been reported often in the literature and is, for example, the CaCa–CaCa band at 3674.7 cm^{-1} reported by Gottschalk et al. (1999) or the A band at 3675 cm^{-1} reported by Hawthorne et al. (2000). This band arises from the occurrence of Mg at the three M1M1M3 octahedral sites adjacent to the OH residing at the O3 site, and the presence of only Ca at the M4 sites. The small band at 3669 cm^{-1} is referred to as the cummingtonite band in Hawthorne et al. (1997) and is attributed by Gottschalk et al. (1999) to the presence of at least three Mg atoms residing at the four M4 sites closest to the O3 (OH) site. The nomenclature of Hawthorne et al. (2000) will be adopted in this study.

The lower three spectra are from Ga-bearing amphiboles with their gallium contents indicated on the figure (nearly constant at 0.3 apfu). Each of the Ga-bearing spectra has the same strong A band at 3674 cm^{-1} (no significant shift in wavenumber) as the Ga-free amphibole, but this band has a noticeable (~30%) reduction in intensity with increasing Ga content. The small cummingtonite band is still perceptible but becomes broader and merges with the dominant A band in the Ga-bearing samples. The reduction in band intensity apparently

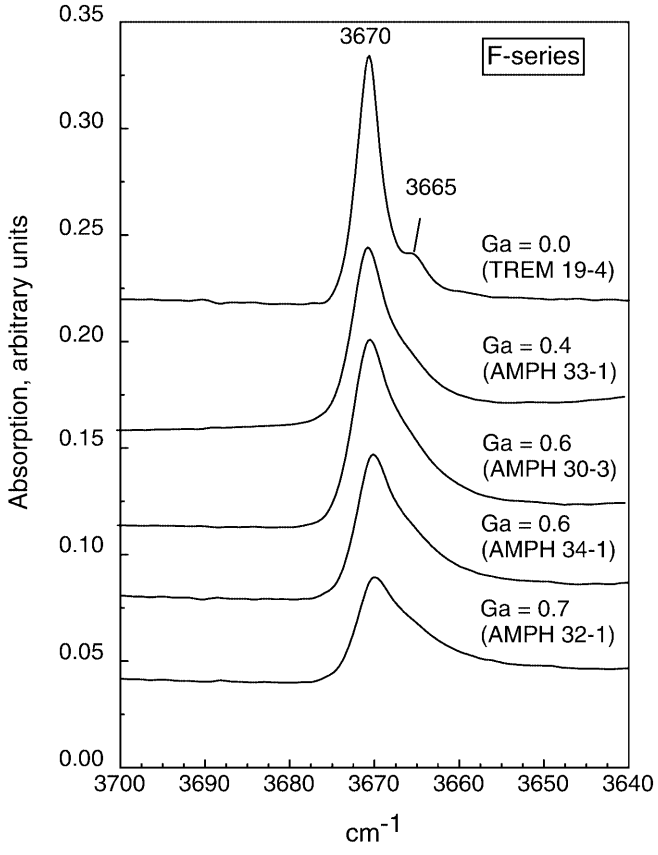

Fig. 9 Infrared spectra in the region of the OH-stretching wavenumber for amphiboles synthesized in the F series. All spectra are plotted at the same scale but offset for clarity. The observed Ga contents (apfu) and sample codes are listed *to the right of each spectrum*. Note the pronounced reduction in intensity and broadening of the bands with increasing Ga content

reflects the antithetic relationship between Ga and OH^- that was noted previously by Jenkins and Hawthorne (1995); however, it is not clear what is substituting for the OH^- to maintain charge balance within the crystal structure. There may be minor replacement of two OH^- with one O^{-2}, but there is no direct evidence in this study to support this hypothesis. The merging of the dominant A band and the small cummingtonite band may be caused either by a broadening effect related to the small amount of Ga residing randomly over some of the M2 and T1 sites, or the appearance of a distinct A band due to Ga at the next-nearest-neighbor M2 site but occurring at a wavenumber between the A and cummingtonite bands (perhaps at 3671 cm^{-1}). There is insufficient range in the Ga content of the OH-bearing amphiboles formed here to discriminate between these two hypotheses.

Fluorine-series syntheses

Rather surprisingly, the fluorine-series amphiboles have a weak but readily identified OH-stretching vibration at a value of 3670 cm^{-1}, as seen in the Ga-free F-tremolite spectrum in the lower part of Fig. 8. This band appears even though the starting mixture was roasted at about 600 °C just prior to being sealed in the capsule. Apparently, trace amounts of hydrogen, from either the pressure medium or from moisture still adhering to the starting mixture, are readily incorporated into the fluorine-rich amphiboles. By simple analogy with the OH-rich amphiboles, the band at 3670 cm^{-1} in F-tremolite must be the A band, and the very weak band at 3665 cm^{-1} appears to be a cummingtonite band. Both of these bands are shifted about 5 cm^{-1} to lower wavenumbers compared to the OH-rich amphiboles, which is in agreement with the sense of shift (to lower wavenumbers) if not magnitude of shift (5–15 cm^{-1}) observed by Robert et al. (1989) for F-bearing richterites and by Robert et al. (2000) for F-bearing pargasites. This does not, however, agree with the study of Robert et al. (1999), who did not observe any shift in band wavenumber with the substitution of up to 1.6 F apfu into OH-bearing tremolite, only a decrease in band intensity.

One can see an inverse correlation between the Ga content and the intensity of the OH-stretching band in the spectra shown in Fig. 9, such that fluor-tremolite (TREM 19-4) has the strongest band and the most gallium-rich amphibole (AMPH 32-1) has the weakest. This re-inforces the antithetic relationship between Ga and OH content noted earlier and is consistent with the very limited amount of Ga substitution observed in this study for the hydroxyl-series amphiboles. These spectra closely parallel those shown in Fig. 7 for the OH-series amphiboles, such that there is a steady decrease in the intensity of the A band and a merging of the A and cummingtonite bands. In this case, the decrease in OH-band intensity is readily explained by the increasing substitution of F^- for OH^- (Table 2). The band broadening or merging is, presumably, caused by the same factors as for the OH-series amphiboles.

We have not observed in the IR spectra of these samples the presence of a lower-frequency B (~3655 cm^{-1}) or C (~3625 cm^{-1}) band attributed primarily to the presence of Ga at the T1 site or Ga at the M3 sites, respectively, as reported for aluminous tremolites by Hawthorne et al. (2000). The absence of the B band in the OH-series amphiboles is attributed to the low concentration of Ga at the T1 sites (~0.1 Ga apfu), which is much less than the lowest Al-contented amphibole (0.8 Al apfu) investigated by Hawthorne et al. (2000). The Ga content of the F-series amphiboles is probably high enough (~0.7 Ga apfu) to observe a B band; however, the very low intensity of the OH-stretching bands in the F-series amphiboles may preclude its detection. One would not expect to see a C band in any of the amphiboles studied here because of the absence of Ga at the M3 (or M1) sites (Table 5).

Discussion

Several key observations have come from the investigation of the tschermak-type substitution into

tremolitic amphibole using Ga as an analogue for Al. First, the hydroxyl-series amphiboles show that Ga does indeed substitute into the structure according to the tschermak substitution, as verified by electron-microprobe analyses, but that the total amount of Ga is at a very small amount (~0.3 Ga apfu). The limited substitution of Ga into the structure is apparently inherent in the tschermak substitution, where earlier studies of the Al-tschermak substitution (e.g., Jenkins 1988; Cho and Ernst 1991; Smelik et al. 1994) indicated maximum levels of about 1.8 Al apfu, considerably less than the theoretical limit of 4 apfu. With Ga the substitution is apparently more limited.

Second, about twice as much Ga (~0.6 apfu) can be incorporated into tremolitic amphibole in the fluorine-series syntheses compared to the hydroxyl series. This increased substitution of Ga is directly related to the presence of F^- instead of OH^- anions in the structure. Although the level of Ga substitution is greater in the fluorine series, the substitution mechanism is *not* via the tschermak substitution but rather a proposed Ca-pargasite substitution which combines a Ga analogue of the tschermak substitution ($^{[6]}Ga^{3+} + {}^{[4]}Ga^{3+} = {}^{[6]}Mg^{2+} + {}^{[4]}Si^{4+}$) with a Ca-equivalent of the edenite substitution ($^{[4]}Ga^{3+} + 1/2{}^{[A]}Ca^{2+} = {}^{[4]}Si^{4+} + 1/2{}^{[A]}\square$) to give the Ca-pargasite substitution of $^{[6]}Ga^{3+} + 2{}^{[4]}Ga^{3+} + 1/2{}^{[A]}Ca^{2+} = {}^{[6]}Mg^{2+} + 2{}^{[4]}Si^{4+} + 1/2{}^{[A]}\square$. This substitution will give the 1:2 ratio of octahedral to tetrahedral Ga observed for the fluorine series (Fig. 4).

The direct correlation between Ga and F content for the tschermakitic amphiboles made in this study and for the pargasitic amphiboles studied by Jenkins and Hawthorne (1995) may point to a more general correlation that exists for other Ca–Al-bearing silicates. For example, minor Al and F has been shown to substitute into titanite ($CaTiOSiO_4$) in a nearly one-to-one correlation (Franz and Spear 1985; Enami et al. 1993; Markl and Piazolo 1999). The presence of the hydroxyl anion has also been clearly documented in titanite by infrared spectroscopy (Hammer et al. 1996); however, the inverse correlation between Ga and OH content observed in the present study has not been so clearly documented for Al and OH in titanite. Indeed, the thermochemical factors controlling the relative contents of Al, F, and OH in titanite have been a source of considerable debate, since field evidence gives conflicting results (Markl and Piazolo 1999). In this study, the amphiboles (of a given series) have all been made under the same pressure and temperature conditions and in the presence of either excess water (hydroxyl series) or trace water (fluorine series) that is presumably at a constant (background) level. What is quite clear is that Ga and F must enter the amphibole structure as a coupled substitution with F gradually excluding OH. In this case, the F and OH contents are directly linked to the Ga content of the starting mixture and not dependent on the ambient partial pressures of either F or OH. This observation supports the hypothesis of Markl and Piazolo (1999) that the F and/or OH content of titanite is controlled by the bulk composition (Al content) of the host rock. Even though the structure of titanite is fundamentally different from amphibole, the direct chemical correlation between Ga and F in amphibole and Al and F in titanite at the macroscopic scale is at least suggestive of some common structural control at the microscopic level that might also exist in other minerals. A complete analysis of the structural origin of this correlation is beyond the scope of this article.

One additional hypothesis that can be tested with the Ga-bearing amphiboles formed in this study is that Al substitutes onto only a subset of the T1 tetrahedral sites in tschermakitic amphiboles. This hypothesis is summarized by Holland and Powell (1998), who note that the phase equilibria involving aluminous tremolitic amphiboles in the system $CaO–MgO–Al_2O_3–SiO_2–H_2O$ (Jenkins 1994; Hoschek 1995) is best modeled by thermodynamic activity expressions that involve random mixing of Al and Mg on the M2 sites but less than random mixing of Al and Si on the T1 sites. If such "partial order" on the T1 sites occurs with long-range order, perhaps driven by avoidance of Al–O–Al (or the equivalent Ga–O–Ga) linkages, this may be present and detectible in the gallium analogues formed in this study. We hasten to point out that long-range order is not required for the activity models, but is at least a testable hypothesis by refining Ga-rich amphiboles in the space group $P2/a$. This was attempted for the amphibole in AMPH 30-3 using the initial atomic coordinates for joesmithite (the only known amphibole with $P2/a$ symmetry) reported by Moore et al. (1993). It was clear that the powder pattern did not have the larger number of reflections that are expected for this lower-symmetry space group, and a complete refinement where all parameters were released could never be accomplished. If one forces the structure to be in the $P2/a$ structure and refines only the site occupancies of the tetrahedral and octahedral sites, there is a weak preferential partitioning of Ga into the T1B and T2B sites (nomenclature of Hawthorne 1983), but these results must be considered suspect. There does not appear to be any clear long-range ordering of Ga onto a particular subset of the tetrahedral sites.

Acknowledgements The authors appreciate the help of W. H. Blackburn with the electron microprobe analyses and J. W. Bell for assistance with FTIR file conversions. Reviews of the manuscript by F. C. Hawthorne, J.-L. Robert, and an anonymous reviewer are gratefully acknowledged. This research was funded by NSF grant EAR-9628212 to DMJ.

References

Barbier J (1998) Crystal structures of sapphirine and surinamite analogues in the $MgO–Ga_2O_3–GeO_2$ system. Eur J Mineral 10: 1283–1293

Cao R-L, Ross C, Ernst WG (1986) Experimental studies to 10 kb of the bulk composition $tremolite_{50}$–$tschermakite_{50}$ + excess H_2O. Contrib Mineral Petrol 93: 160–167

Cho M, Ernst WG (1991) An experimental determination of calcic amphibole solid solution along the join tremolite–tschermakite. Am Mineral 76: 985–1001

Enami M, Suzuki K, Liou JG, Bird DK (1993) Al–Fe^{3+} and F–OH substitutions in titanite and constraints on their *P–T* dependence. Eur J Mineral 5: 219–231

Franz G, Spear FS (1985) Aluminous titanite (sphene) from the eclogite-zone, south-central Tauern Window, Austria. Chem Geol 50: 33–46

Gottschalk M, Andrut M, Melzer S (1999) The determination of the cummingtonite content of synthetic tremolite. Eur J Mineral 11: 967–982

Hammer VMF, Beran A, Endisch D, Rauch F (1996) OH concentration in natural titanites determined by FTIR spectroscopy and nuclear reaction analysis. Eur J Mineral 8: 281–288

Hawthorne FC (1983) The crystal chemistry of the amphiboles. Can Mineral 21: 173–480

Hawthorne FC (1997) Short-range order in amphiboles: a bond-valence approach. Can Mineral 35: 201–216

Hawthorne FC, Della Ventura G, Robert J-L, Welch MD, Raudsepp M, Jenkins DM (1997) A Rietveld and infrared study of synthetic amphiboles along the potassium-richterite-tremolite join. Am Mineral 82: 708–716

Hawthorne FC, Welch MD, Della Ventura G, Robert J-L, Jenkins DM (2000) Short-range order in synthetic aluminous tremolites: an infrared and triple-quantum MAS NMR study. Am Mineral 85: 1716–1724

Holland TJB, Powell R (1998) An internally consistent thermodynamic data set for phases of petrological interest. J Metamorphic Petrol 16: 309–343

Hoschek G (1995) Stability relations and Al content of tremolite and talc in CMASH assemblages with kyanite + zoisite + quartz + H_2O. Eur J Mineral 7: 353–362

Jenkins DM (1987) Synthesis and characterization of tremolite in the system H_2O–CaO–MgO–SiO_2. Am Mineral 72: 707–715

Jenkins DM (1988) Experimental study of the join tremolite–tschermakite: a reinvestigation. Contrib Mineral Petrol 99: 392–400

Jenkins DM (1994) Experimental reversal of the aluminum content in tremolitic amphiboles in the system H_2O–CaO–MgO–Al_2O_3–SiO_2. Am J Sci 294: 593–620

Jenkins DM, Hawthorne FC (1995) Synthesis and Rietveld refinement of amphibole along the join $Ca_2Mg_5Si_8O_{22}F_2$–$NaCa_2Mg_4Ga_3Si_6O_{22}F_2$. Can Mineral 33: 13–24

Jenkins DM, Sherriff BL, Cramer J, Xu Z (1997) Al, Si, and Mg occupancies in tetrahedrally and octahedrally coordinated sites in synthetic aluminous tremolites. Am Mineral 82: 280–290

Konopásek J (1998) Formation and destabilization of the high pressure assemblage garnet–phengite–paragonite (Krušné hory Mountains, Bohemian Massif): the significance of the Tschermak substitution in the metamorphism of pelitic rocks. Lithos 42: 269–284

Levien L, Prewitt CT (1981) High-pressure structural study of diopside. Am Mineral 66: 315–323

Markl G, Piazolo S (1999) Stability of high-Al titanite from low-pressure calcsilicates in light of fluid and host-rock composition. Am Mineral 84: 37–47

Moore PB, Davis AM, Van Derveer DG, Sen Gupta PK (1993) Joesmithite, a plumbous amphibole revisited and comments on bond valences. Mineral Petrol 48: 97–113

Oba T (1978) Phase relationship of $Ca_2Mg_3Al_2Si_6Al_2O_{22}(OH)_2$–$Ca_2Mg_3Fe^{3+}{}_2Si_6Al_2O_{22}(OH)_2$ join at high temperature and high pressure – the stability of tschermakite. J Fac Sci Hokkaido Univ 18: 339–350

Oberti R, Hawthorne FC, Ungaretti L, Cannillo E (1995a) $^{[6]}$Al disorder in amphiboles from mantle peridotites. Can Mineral 33: 867–878

Oberti R, Ungaretti L, Cannillo E, Hawthorne FC, Memmi I (1995b) Temperature-dependent Al order-disorder in the tetrahedral double-chains of *C*2/*m* amphiboles. Eur J Mineral 7: 1049–1063

Oberti R, Hawthorne FC, Raudsepp M (1997) The behavior of Mn in amphiboles: Mn in synthetic fluor-edenite and synthetic fluor-pargasite. Eur J Mineral 9: 115–122

Quirion DM, Jenkins DM (1998) Dehydration and partial melting of tremolitic amphibole coexisting with zoisite, quartz, anorthite, diopside, and water in the system H_2O–CaO–MgO–Al_2O_3–SiO_2. Contrib Mineral Petrol 130: 379–389

Raudsepp M, Hawthorne FC, Turnock AC (1990) Evaluation of the Rietveld method for the characterization of fine-grained products of mineral synthesis: the diopside–hedenbergite join. Can Mineral 28: 93–109

Robert J-L, Della Ventura G, Thauvin J-L (1989) The infrared OH-stretching region of synthetic richterites in the system Na_2O–K_2O–CaO–MgO–SiO_2–H_2O–HF. Eur J Mineral 1: 203–211

Robert J-L, Della Ventura G, Hawthorne FC (1999) Near-infrared study of short-range disorder of OH and F in monoclinic amphiboles. Am Mineral 84: 86–91

Robert J-L, Della Ventura G, Welch MD, Hawthorne FC (2000) The OH-F substitution in synthetic pargasite at 1.5 kbar, 850 °C. Am Mineral 85: 926–931

Roots M (1995) Tschermak substitution in the assemblage muscovite + biotite + chlorite + quartz: a comparison between natural and thermodynamic data. N Jahrb für Mineral Monats pp 75–95

Sasaki S, Takeuchi Y, Fujino K, Akimoto S (1982) Electron-density distributions of three orthopyroxenes, $Mg_2Si_2O_6$, $Co_2Si_2O_6$, and $Fe_2Si_2O_6$. Z Kristallogr 158: 279–297

Smart RM, Glasser FP (1978) Phase formation in the system MgO–Ga_2O_3–SiO_2. J Mater Sci 13: 671–674

Smelik EA, Jenkins DM, Navrotsky A (1994) A calorimetric study of synthetic amphiboles along the tremolite-tschermakite join and the heats of formation of magnesiohornblende and tschermakite. Am Mineral 79: 1110–1122

Stephenson D (1993) Amphiboles from Dalradian metasedimentary rocks of the NE Scotland: environmental inferences and distinction from amphiboles of meta-igneous amphibolites. Mineral Petrol 49: 45–62

Stormer JC Jr, Pierson ML, Tacker RC (1993) Variation of F and Cl X-ray intensity due to anisotropic diffusion in apatite during electron microprobe analysis. Am Mineral 78: 641–648

Young RA, Sakthivel A, Moss TS, Paiva-Santos CO (1994) User's guide to program DBWS-9411. Georgia Institute of Technology, Atlanta, Georgia, 60 p

Zingg AJ (1993) Intra- and intercrystalline cation-exchange reactions in zoned calcic amphibole from the Bushveld complex. Can Mineral 31: 649–663